Supporting Information

Pressurized Formic Acid Dehydrogenation: An Entropic Spring Replaces Hydrogen Compression Cost

Van K. Do[a], Nicolas Alfonso Vargas[a], Anthony J. Chavez[a], Long Zhang[a], Valeriy Cherepakhin[a], Zhiyao Lu[a], Robert P. Currier[b], Pavel A. Dub[b], John C. Gordon[c], and Travis J. Williams*[a]

[a] Loker Hydrocarbon Research Institute, Wrigley Institute for Environmental Studies, and Department of Chemistry, University of Southern California, Los Angeles, California, 90089, USA.

[b] Chemistry Division, Los Alamos National Laboratory, Los Alamos, New Mexico 87545, United States.

[c] National Security Education Center (NSEC), Los Alamos National Laboratory, Los Alamos,

New Mexico 87545, United States

Table of Contents

1. Theoretical Yield & Reaction Rate Calculations

Based on the Ideal gas law equation and assuming 100% FA conversion from 3.00 mL (79.5 mmol) of FA, we would yield:

a. <u>Ambient Pressure:</u>

$n_{evolved\ gases}$ = 159 mmol

P = 1 atm

R = 0.08206 L atm K^{-1} mol^{-1}

T = 25 °C + 273 = 298 K

V = (n • R • T) / P = 3.89 Liter

FA conversion % = ($V_{evolved\ gas}$ / 3.89)*100

b. <u>Self-Pressurized Conditions:</u>

$n_{evolved\ gases}$ = 0.159 mol

R = 0.08206 L atm K^{-1} mol^{-1}

T = 110°C + 273.15 = 383.15 K

V = 0.125 L

P = (n • R • T) / V = 39.99 atm = 40.5 bar

High-pressure H_2/CO_2 mixtures cannot be precisely predicted by either the Ideal Gas Law or the Van der Waals' equation of state, therefore, we utilized the best catalytic run (table 1, entry 11) to be our standard 100% FA conversion yield. ^{1}H NMR at the end of entry 11 suggested there was no trace of unreacted FA left. Therefore, under self-pressurized condition conversion was calculated by:

FA conversion % = ($P_{evolved\ gas}$ /38 bar)*100

All volumetric rate data is always expressed in normal liters per hour, (L/hr) standardized to 0 °C and 1 atm. An example calculation of a volumetric rate from pressure is shown below:

P_1 = 990 psi; T_1 = 118 °C

P_2 = 1005 psi; T_2 = 120 °C

V = 600 mL

Δt = 8 s

$\Delta n = [P_2 / (273.15\ K + T_2) - P_1 / (273.15\ K + T_1)] / 14.7 \bullet V / 1000 / R$

Rate (L/hr) = $\Delta n \bullet R \bullet 273.15\ K / 1\ atm / (\Delta t / 3600)$ = 126.8 L/hr

2. Synthesis and characterizations of Complex **11-CO** and **5**

Complex **11-CO**: A solution of complex **11** (200 mg, 2.91 x 10^{-4} mol) and sodium formate (99 mg, 1.46 mmol, 5 eq.) in formic acid (20 mL) was stirred at room temperature under nitrogen for one hour. When the solution became yellow, it was heated in an oil bath for 4 hours at 90 ^{o}C. Then, the temperature was raised to 115 ^{o}C and the remaining formic acid was distilled off affording a red solid. The solid was extracted with CH_2Cl_2, filtered, and the resulting black-red solution was diluted with diethyl ether. The next day the product crystallized as dark-red crystals. They were filtered, washed with diethyl ether, and dried in vacuum (118 mg, 71%).

^{1}H NMR (500 MHz, CD_2Cl_2): δ 9.74 (d, *J* = 5.3 Hz, 2H, ArH), 7.96 (t, *J* = 7.6 Hz, 2H, ArH), 7.77 (d, *J* = 7.7 Hz, 2H, ArH), 7.28 (t, *J* = 6.4 Hz, 2H, ArH), 5.33 (s, 2H, CH_2Cl_2), 3.75 (d, *J* = 8.2 Hz, 4H, $2CH_2$), 1.41 (d, *J* = 13.7 Hz, 36H, $12CH_3$), –0.09 (t, $^{2}J_{PH}$ = 56.4 Hz, 1H, IrH).

^{13}C{^{1}H} NMR (126 MHz, CD_2Cl_2): δ 179.13, 166.74, 160.82, 140.51, 124.31, 124.02 (t, *J* = 4.8 Hz), 37.24 – 36.64 (m), 36.21 – 35.76 (m), 29.22.

^{19}F NMR (564 MHz, CD_2Cl_2): δ –78.89.

^{31}P{^{1}H} NMR (243 MHz, CD_2Cl_2): δ 78.06 (s).

IR (KBr, cm^{-1}): 2965, 2905, 2874, 2043, 1960 (ν_{CO}), 1612, 1479, 1274, 1151, 1034, 829, 770, 640.

MALDI-MS: *m/z* calcd for $[C_{30}H_{49}Ir_2N_2O_2P_2]^+$ 915.25, found 915.21.

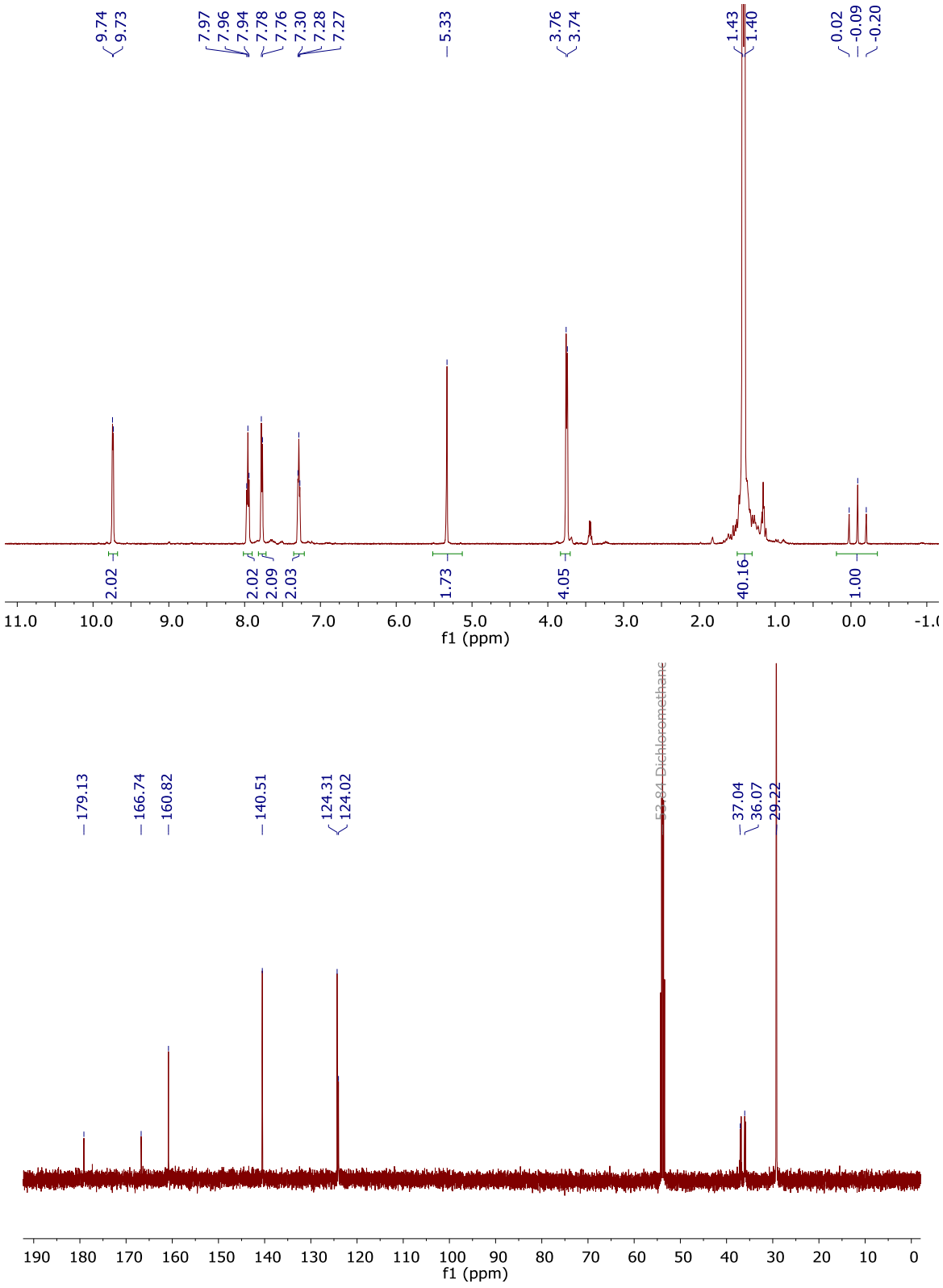

Figure S1. ^{1}H and $^{13}C\{^{1}H\}$ NMR spectra of **11-CO** in CD_2Cl_2.

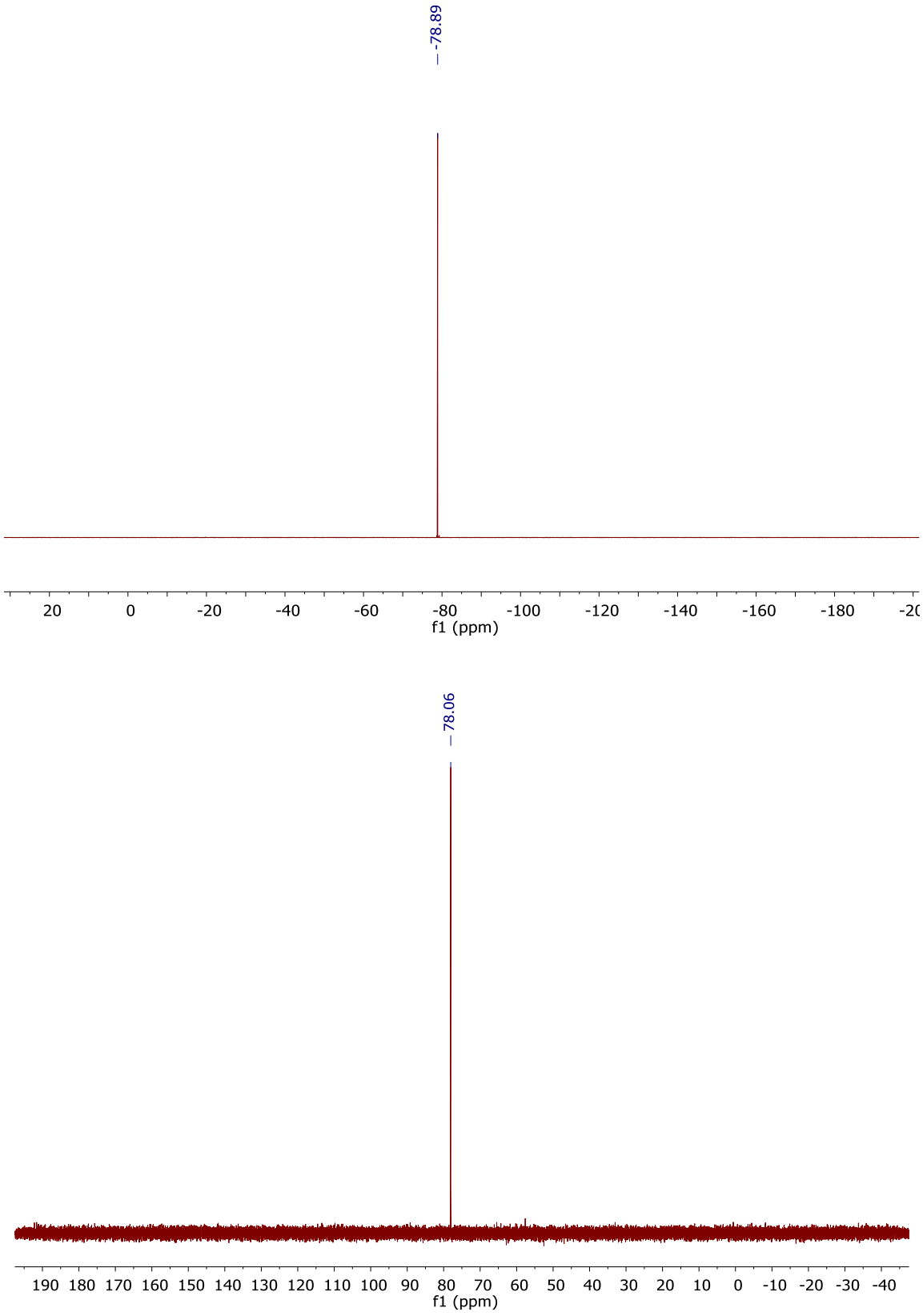

Figure S2. ^{19}F (top) and $^{31}P\{^{1}H\}$ (bottom) NMR spectra of **11-CO** in CD_2Cl_2.

Complex **5**: In a N_2-filled glovebox, a suspension of **4** (200 mg, 0.27 mmol) in toluene (5 ml) was added a solution of $NaHBEt_3$ (1.0 M in toluene; 0.54 mL; 0.54 mmol) dropwise at room temperature. The white suspension slowly turned into a transparent orange-red solution within 1 hour. The reaction was stirring at room temperature for 18 hours giving a dark orange solution. The reaction mixture volume was partially reduced under vacuum and filtered. The resulting filtrate was concentrated under vacuum, layered with pentane in the glovebox to obtain turmeric yellow crystalline solid in 2 days. They were filtered, washed with pentane, and dried in vacuum.

^{1}H NMR (600 MHz, C_6D_6): δ -11.6 (s, 1H, RuH), -7.5 (dd, $^2J_{HH}$ = 18 Hz, 1H, RuH), δ 1.72 (s, 3H), δ 1.86-2.35 (m, 7H), δ 2.97 (d, 2H), δ 6.93-7.12 (m, 12H), δ 7.17-7.32 (m, 4H), δ 7.67 (t, *J* = 7.67 Hz, 8H).

^{31}P{^{1}H} NMR (243 MHz, C_6D_6): δ 78.75 (s), δ 50.94 (s).

MALDI-MS: *m/z* calcd for 669.13, found 669.25.

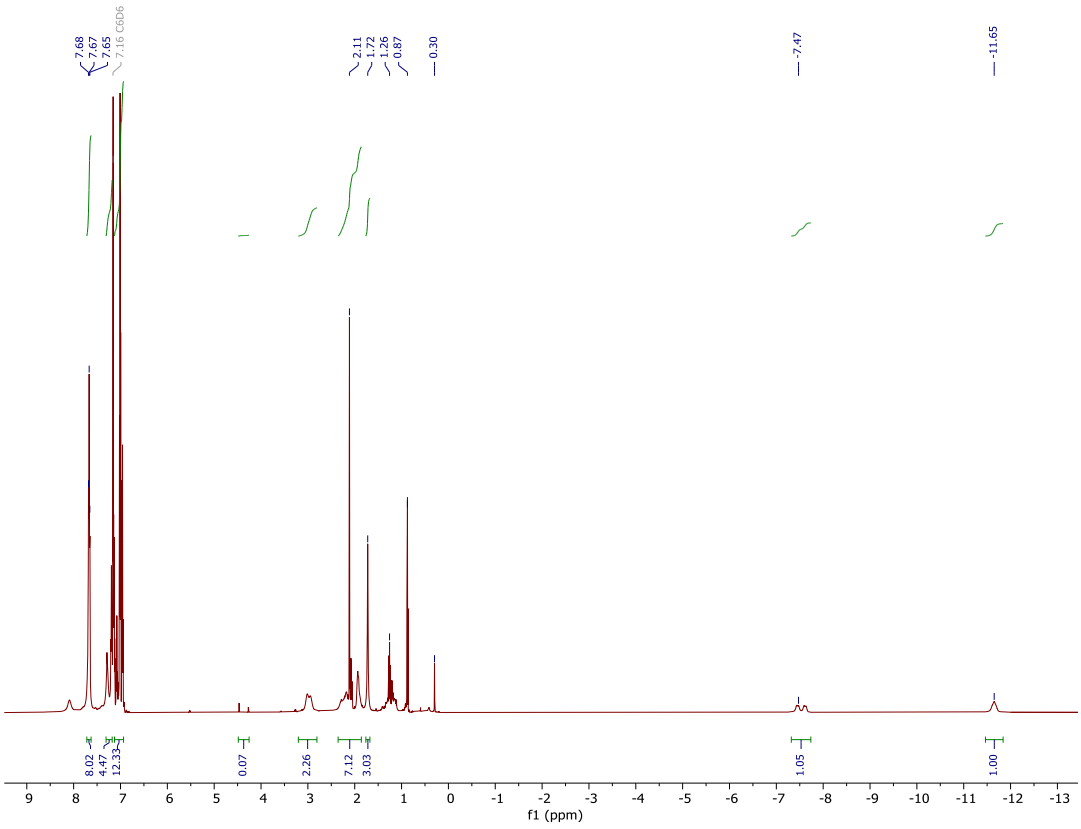

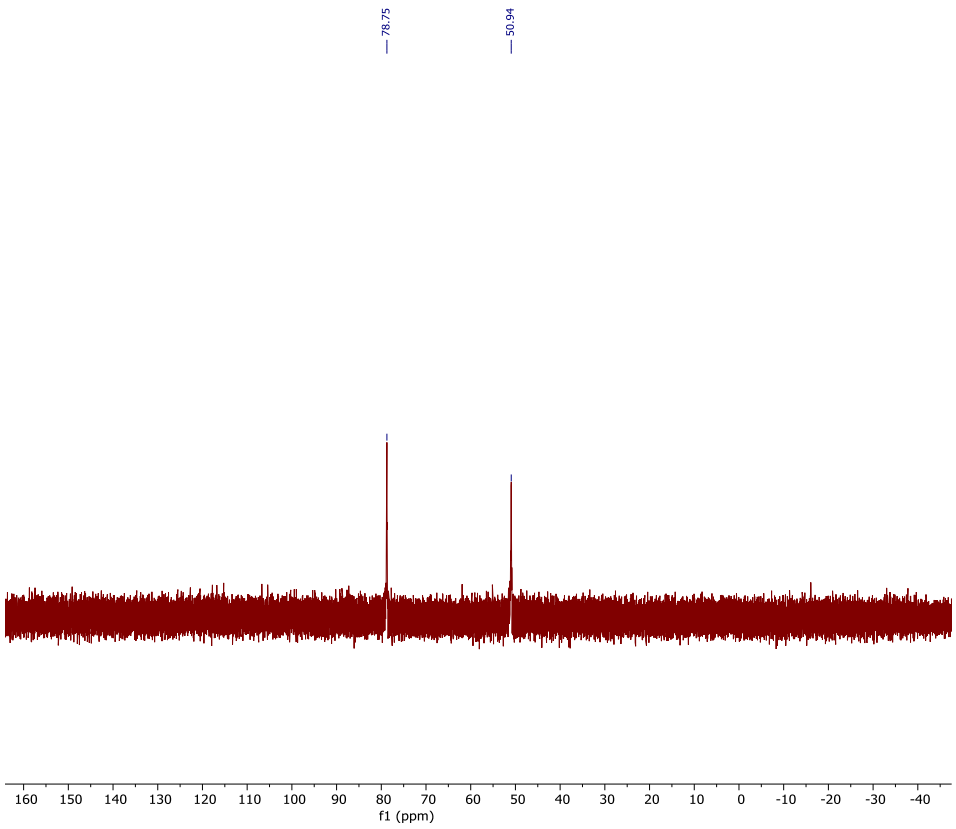

Figure S3. ^{1}H and $^{31}P\{^{1}H\}$ NMR spectra of **5** in C_6D_6.

3. Ambient Pressure Kinetics of All Screened Catalysts

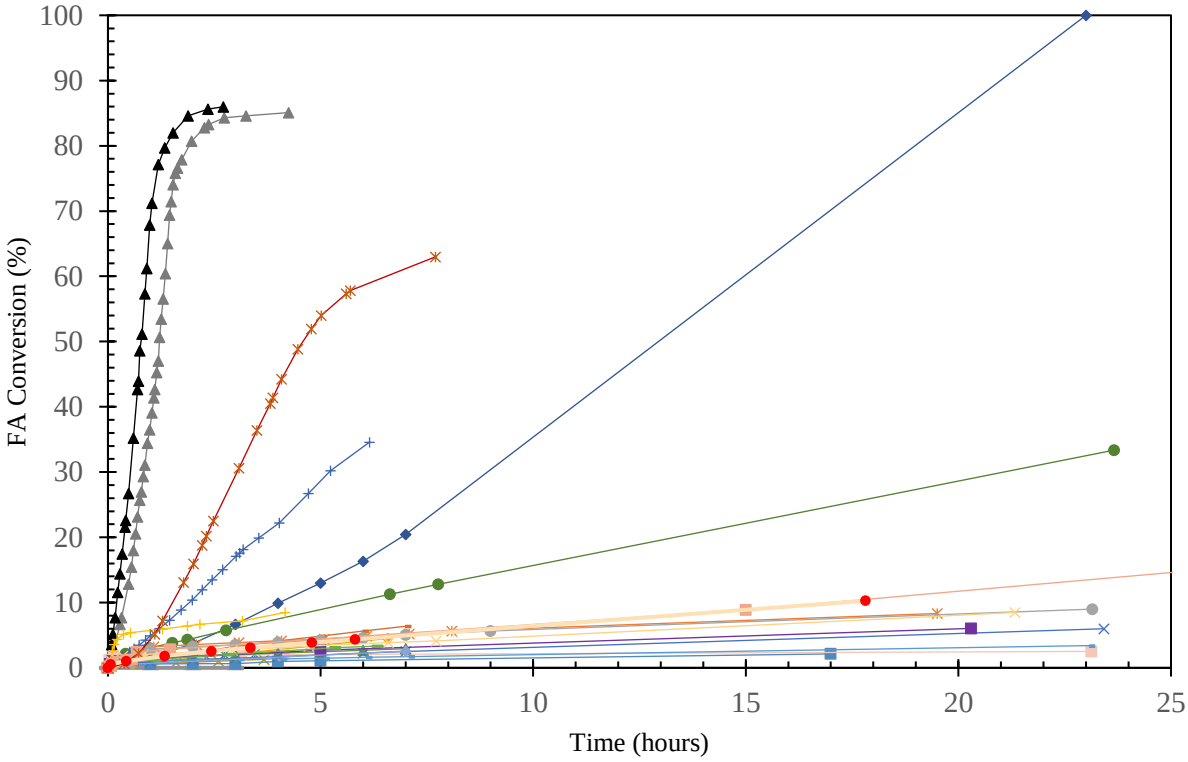

Figure S4a. Gas evolution of formic acid dehydrogenation by complexes **1-21** at ambient pressure over time (0 - 25 hours): complex **1** – lavender crosses; complex 1 w/ ^{t}BuOK – purple squares; complex **2** – orange asterisks; complex **2** w/^{t}BuOK – grey circles; complex **3** – yellow plusses; complex **4** – blue squares; complex **4** w/ ^{t}BuOK – peach squares; complex **5** – green triangles; complex **6** – cream crosses; complex **7** – red asterisks; complex **8** – red circles; complex **9-CO** – blue plusses; complex **10** – orange hyphens; complex **11** – black triangles;–; complex **12** – navy diamonds; complex **13** – grey hyphens; complex **14** – yellow crosses; complex **15** – blue asterisks; complex **16** – lavender diamonds; complex **17** – pink squares; complex **18** – green hyphens; complex **19** – grey triangles; complex **20** –green circles; complex **21** – yellow diamonds

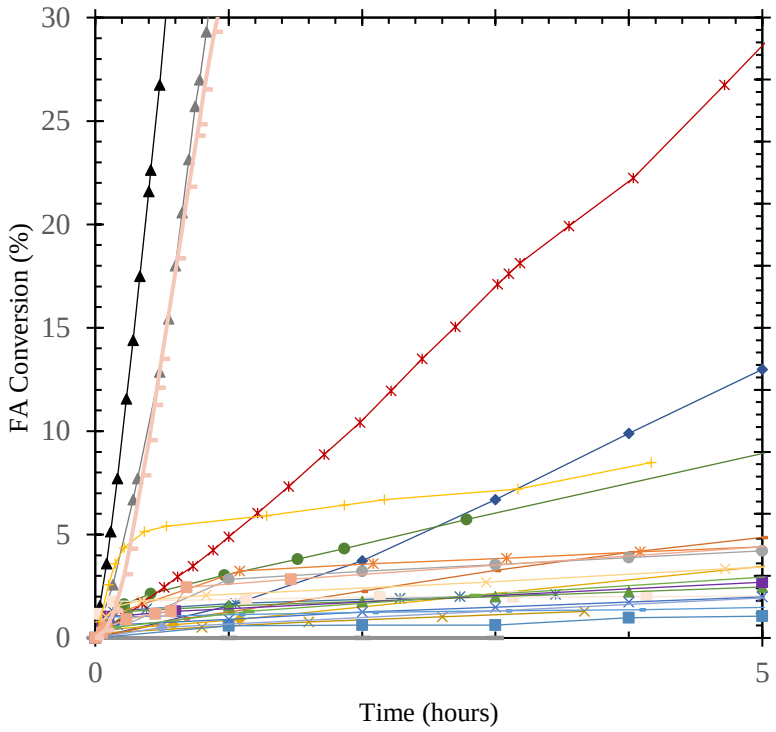

Figure S4b. Gas evolution of formic acid dehydrogenation by complexes **1-20** at ambient pressure over time (0 - 5 hours): complex **1** – lavender crosses; complex 1 w/ ^{t}BuOK – purple squares; complex **2** – orange asterisks; complex **2** w/^{t}BuOK – grey circles; complex **3** – yellow plusses; complex **4** – blue squares; complex **4** w/ ^{t}BuOK – peach squares; complex **5** – green triangles; complex **6** – cream crosses; complex **7** – red asterisks; complex **8** – red circles; complex **9-CO** – blue plusses; complex **10** – orange hyphens; complex **11** – black triangles;–; complex **12** – navy diamonds; complex **13** – grey hyphens; complex **14** – yellow crosses; complex **15** – blue asterisks; complex **16** – lavender diamonds; complex **17** – pink squares; complex **18** – green hyphens; complex **19** – grey triangles; complex **20** –green circles; complex **21** – yellow diamonds

Ambient versus Self-Pressurized Kinetics

All 20 screened catalysts kinetic profile under ambient pressure versus self-pressurized by evolved gases.

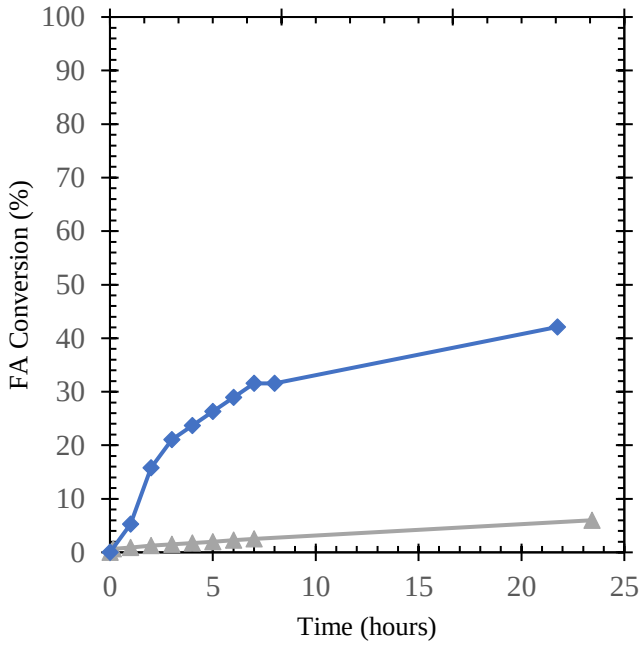

Figure S5. Gas evolution of formic acid dehydrogenation by complex **1** with pre-activation over time at ambient pressure condition (opened system) – grey triangles; at self-pressurized condition (closed system) – blue diamonds.

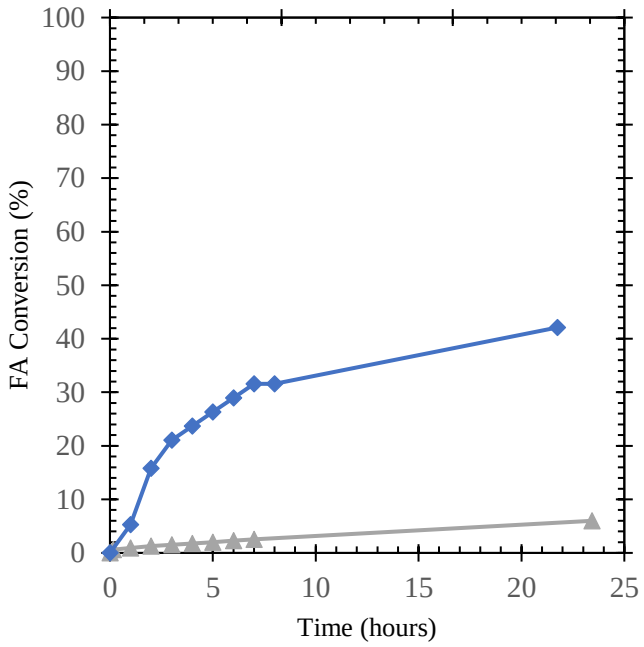

Figure S6. Gas evolution of formic acid dehydrogenation by complex **1** without pre-activation over time at ambient pressure condition (opened system) – grey triangles; at self-pressurized condition (closed system) – blue diamonds.

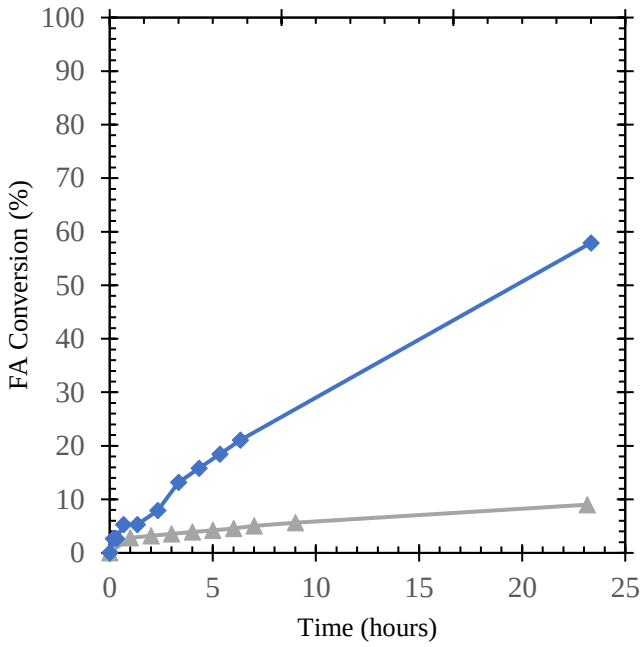

Figure S7. Gas evolution of formic acid dehydrogenation by complex **2** with pre-activation over time at ambient pressure condition (opened system) – grey triangles; at self-pressurized condition (closed system) – blue diamonds.

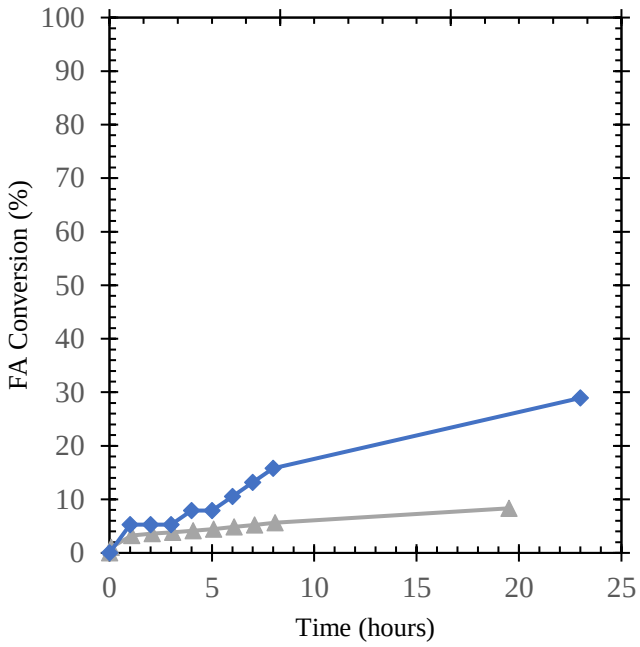

Figure S8. Gas evolution of formic acid dehydrogenation by complex **2** without pre-activation over time at ambient pressure condition (opened system) – grey triangles; at self-pressurized condition (closed system) – blue diamonds.

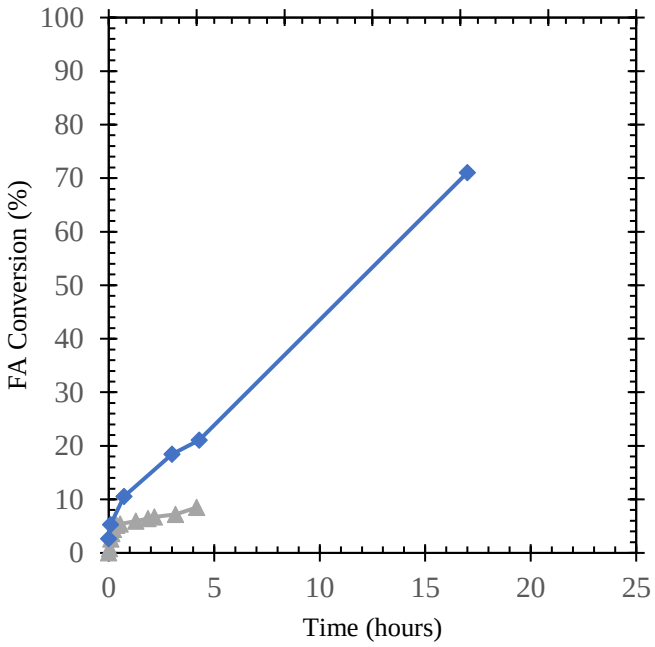

Figure S9. Gas evolution of formic acid dehydrogenation by complex **3** over time at ambient pressure condition (opened system) – grey triangles; at self-pressurized condition (closed system) – blue diamonds.

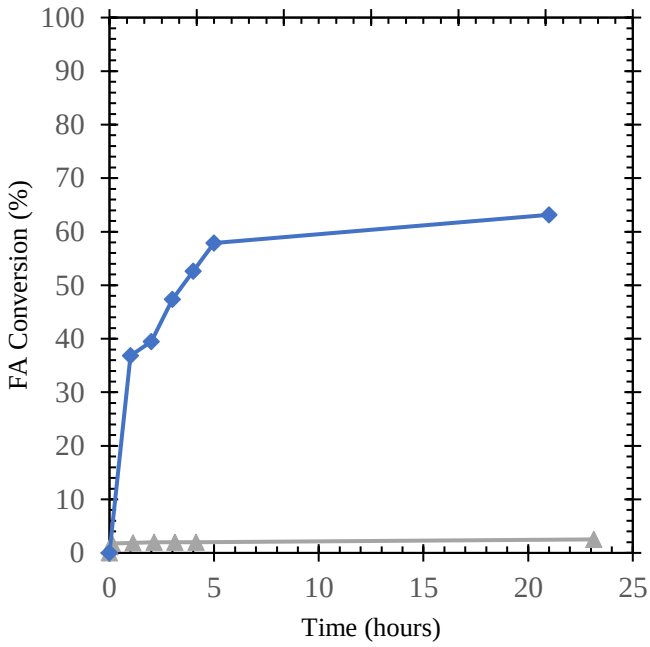

Figure S10. Gas evolution of formic acid dehydrogenation by complex **4** with pre-activation over time at ambient pressure condition (opened system) – grey triangles; at self-pressurized condition (closed system) – blue diamonds.

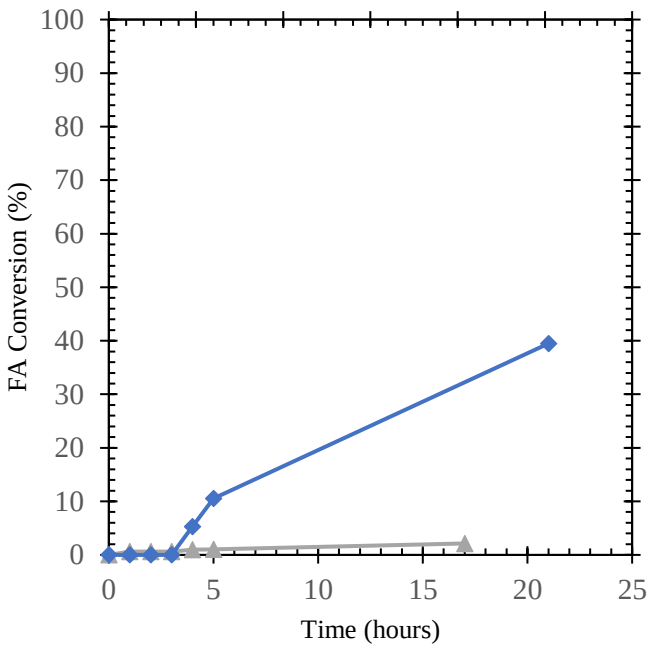

Figure S11. Gas evolution of formic acid dehydrogenation by complex **4** without pre-activation over time at ambient pressure condition (opened system) – grey triangles; at self-pressurized condition (closed system) – blue diamonds.

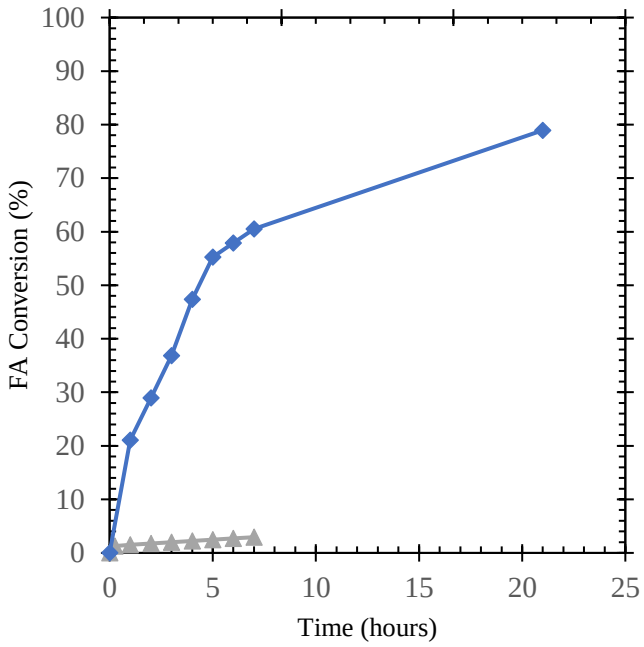

Figure S12. Gas evolution of formic acid dehydrogenation by complex **5** over time at ambient pressure condition (opened system) – grey triangles; at self-pressurized condition (closed system) – blue diamonds.

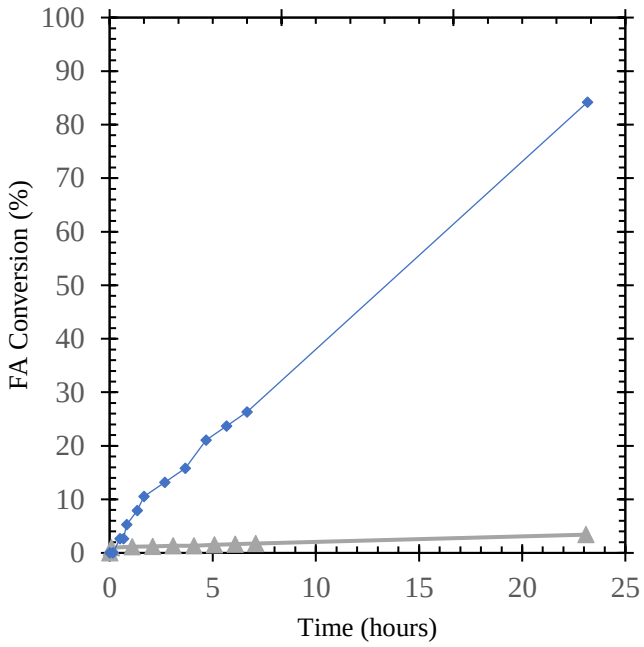

Figure S13. Gas evolution of formic acid dehydrogenation by complex **6** with pre-activation over time at ambient pressure condition (opened system) – grey triangles; at self-pressurized condition (closed system) – blue diamonds. No activity at ambient pressure over 3 hours.

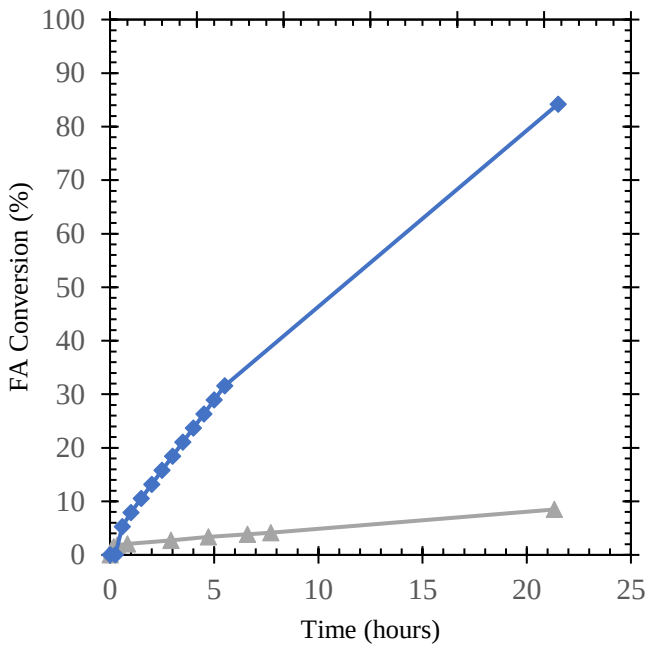

Figure S14. Gas evolution of formic acid dehydrogenation by complex **6** without pre-activation over time at ambient pressure condition (opened system) – grey triangles; at self-pressurized condition (closed system) – blue diamonds.

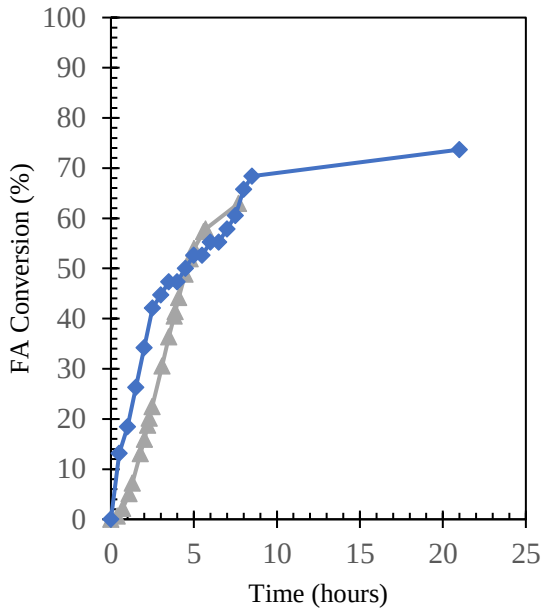

Figure S15. Gas evolution of formic acid dehydrogenation by complex **7** over time at ambient pressure condition (opened system) – grey triangles; at self-pressurized condition (closed system) – blue diamonds.

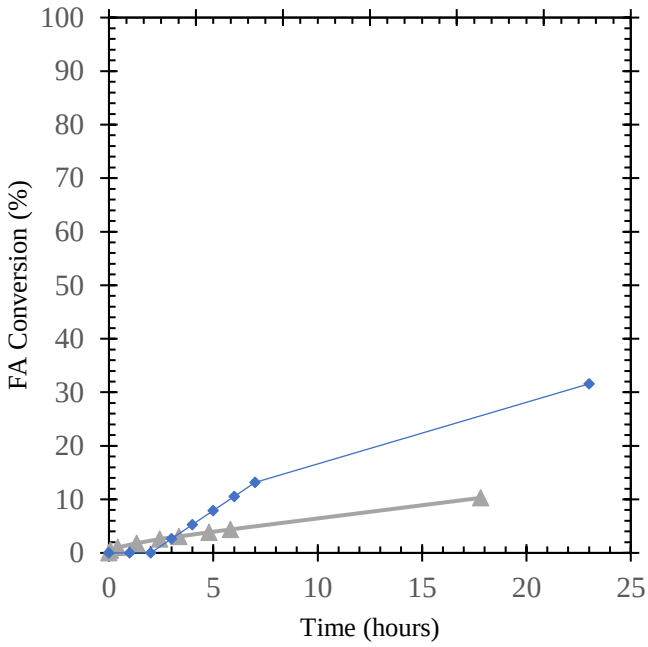

Figure S16. Gas evolution of formic acid dehydrogenation by complex **8** over time at ambient pressure condition (opened system) – grey triangles; at self-pressurized condition (closed system) – blue diamonds.

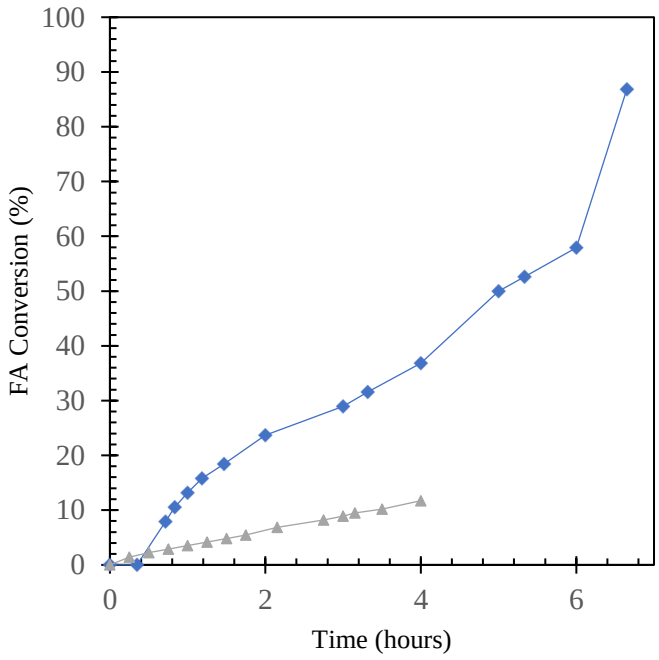

Figure S17. Gas evolution of formic acid dehydrogenation by complex **9** over time at ambient pressure condition (opened system) – grey triangles; at self-pressurized condition (closed system) – blue diamonds.

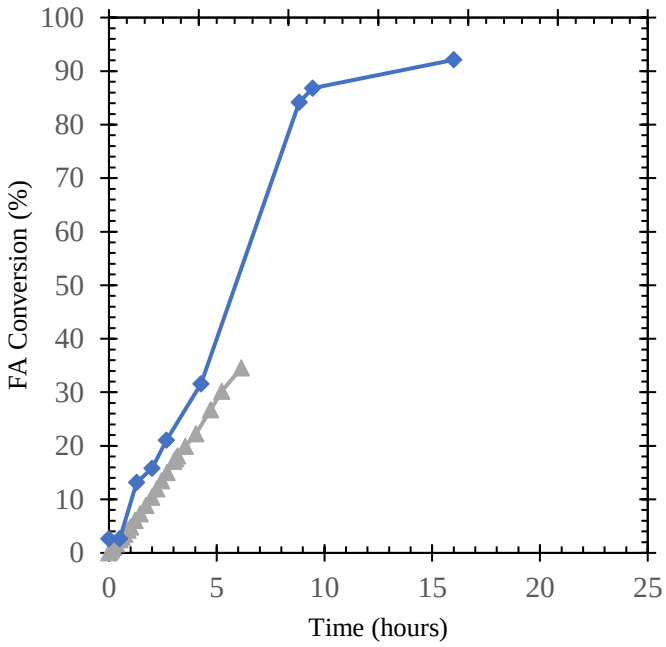

Figure S18. Gas evolution of formic acid dehydrogenation by complex **9-CO** over time at ambient pressure condition (opened system) – grey triangles; at self-pressurized condition (closed system) – blue diamonds.

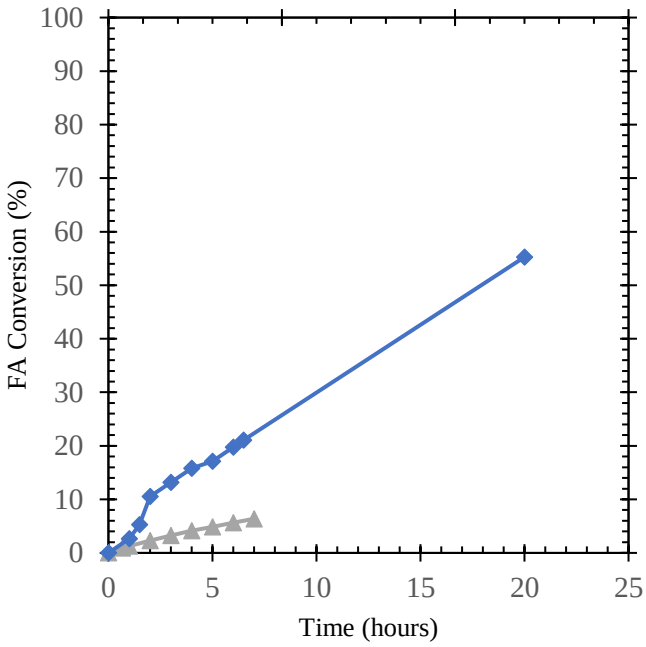

Figure S19. Gas evolution of formic acid dehydrogenation by complex **10** over time at ambient pressure condition (opened system) – grey triangles; at self-pressurized condition (closed system) – blue diamonds.

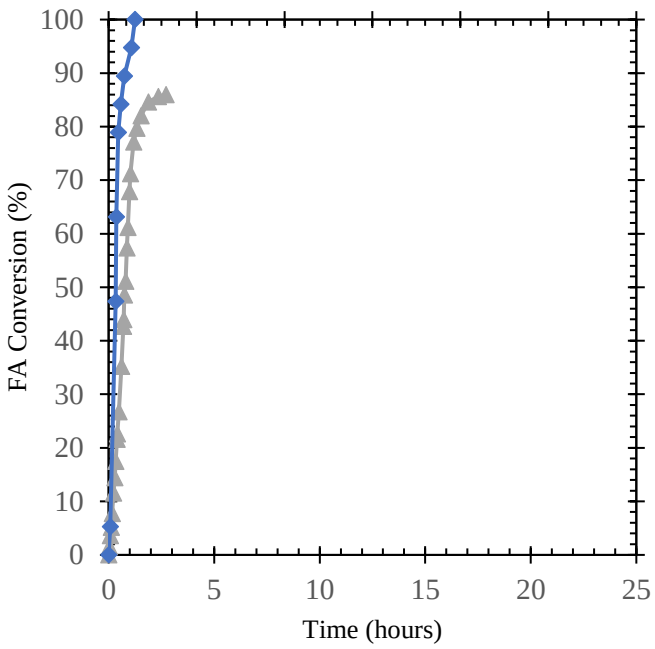

Figure S20. Gas evolution of formic acid dehydrogenation by complex **11** over time at ambient pressure condition (opened system) – grey triangles; at self-pressurized condition (closed system) – blue diamonds.

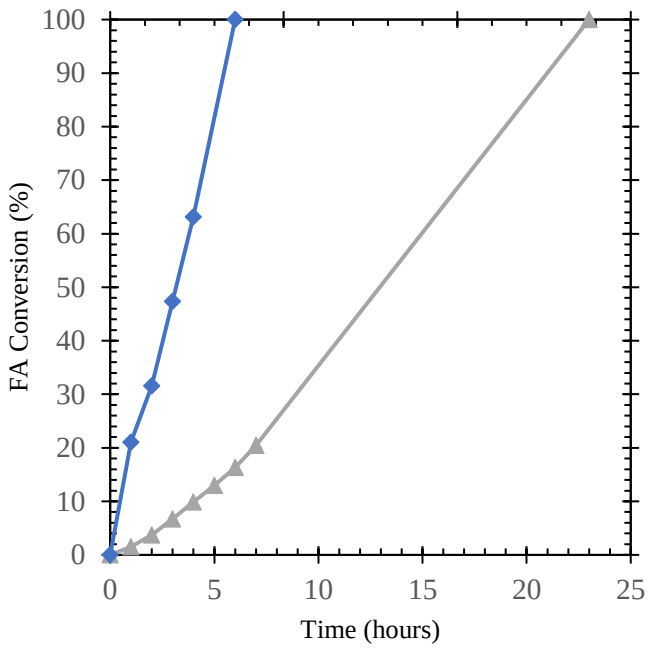

Figure S21. Gas evolution of formic acid dehydrogenation by complex **12** over time at ambient pressure condition (opened system) – grey triangles; at self-pressurized condition (closed system) – blue diamonds.

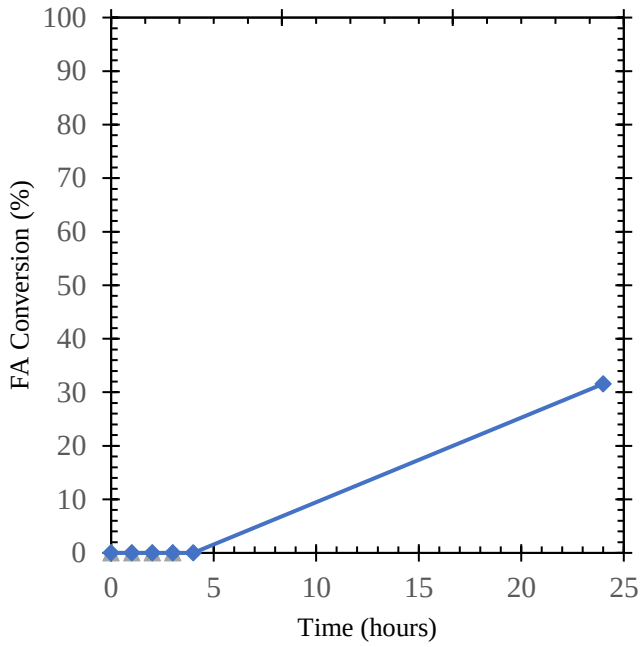

Figure S22. Gas evolution of formic acid dehydrogenation by complex **13** over time at ambient pressure condition (opened system) – grey triangles; at self-pressurized condition (closed system) – blue diamonds.

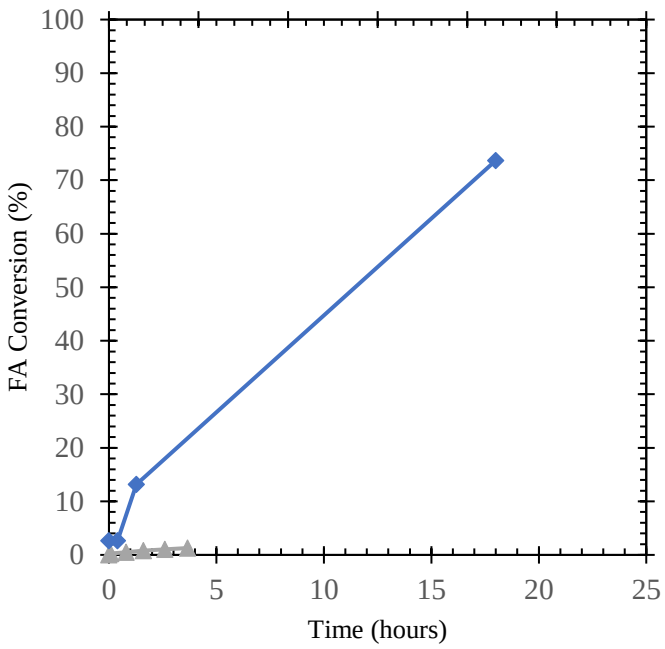

Figure S23. Gas evolution of formic acid dehydrogenation by complex **14** over time at ambient pressure condition (opened system) – grey triangles; at self-pressurized condition (closed system) – blue diamonds.

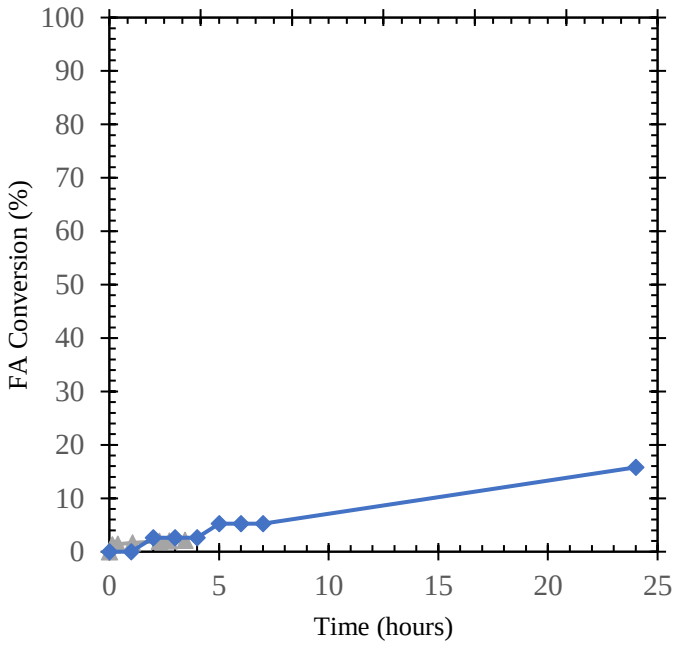

Figure S24. Gas evolution of formic acid dehydrogenation by complex **15** over time at ambient pressure condition (opened system) – grey triangles; at self-pressurized condition (closed system) – blue diamonds.

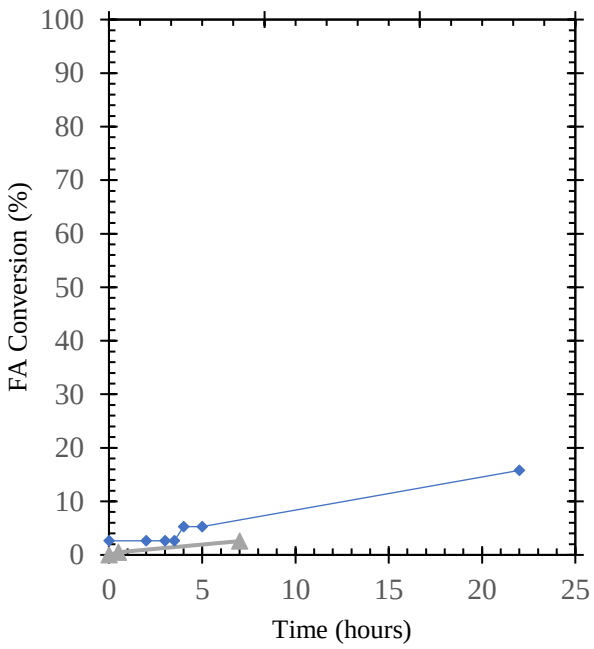

Figure S25. Gas evolution of formic acid dehydrogenation by complex **16** over time at ambient pressure condition (opened system) – grey triangles; at self-pressurized condition (closed system) – blue diamonds.

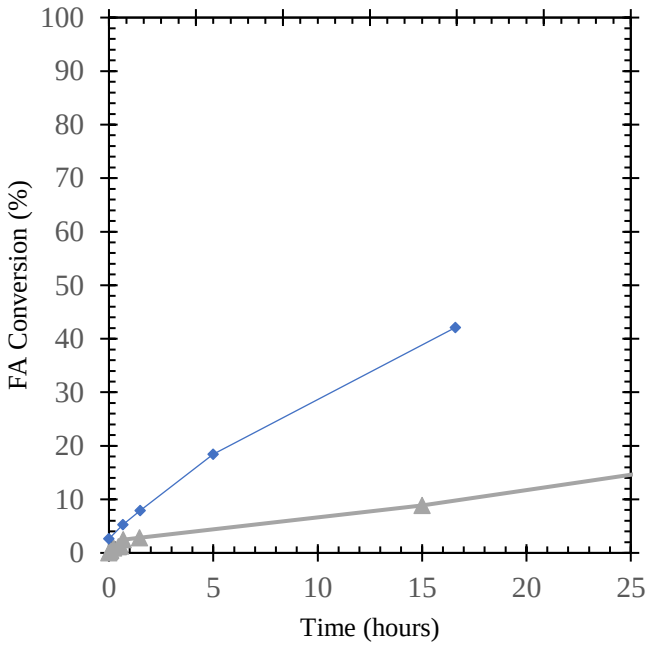

Figure S26. Gas evolution of formic acid dehydrogenation by complex **17** over time at ambient pressure condition (opened system) – grey triangles; at self-pressurized condition (closed system) – blue diamonds.

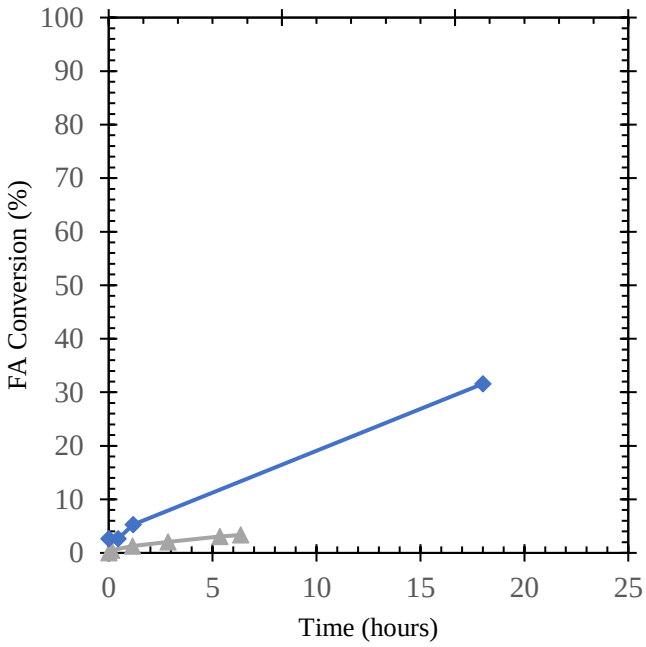

Figure S27. Gas evolution of formic acid dehydrogenation by complex **18** over time at ambient pressure condition (opened system) – grey triangles; at self-pressurized condition (closed system) – blue diamonds.

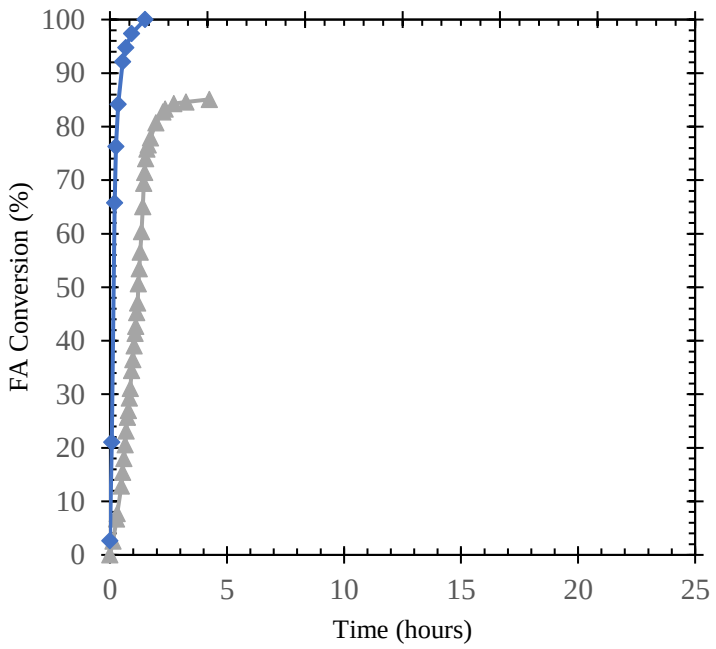

Figure S28. Gas evolution of formic acid dehydrogenation by complex **19** over time at ambient pressure condition (opened system) – grey triangles; at self-pressurized condition (closed system) – blue diamonds.

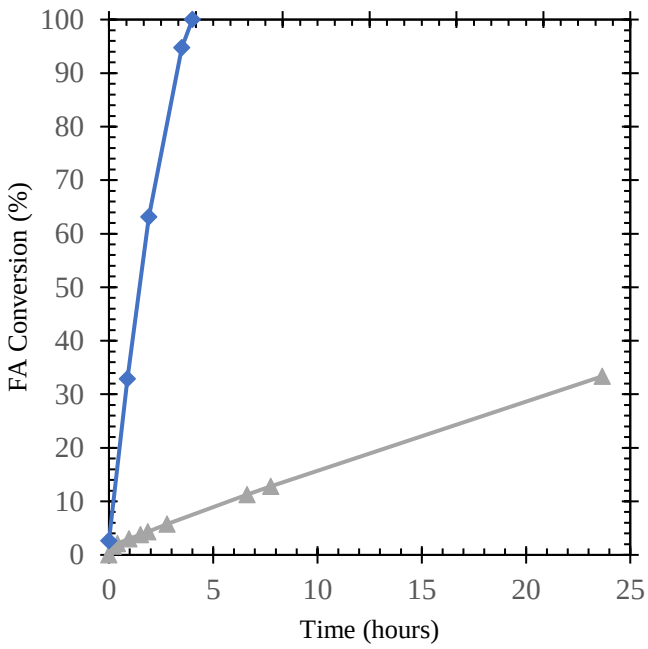

Figure S29. Gas evolution of formic acid dehydrogenation by complex **20** over time at ambient pressure condition (opened system) – grey triangles; at self-pressurized condition (closed system) – blue diamonds.

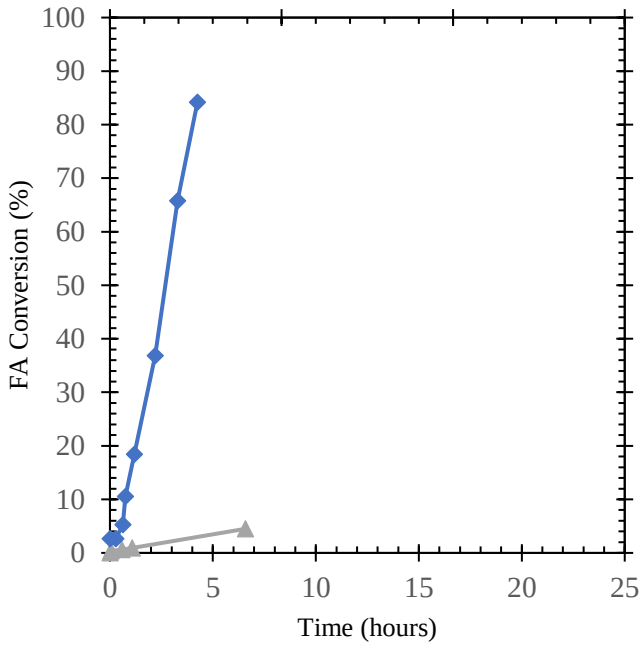

Figure S30. Gas evolution of formic acid dehydrogenation by complex **21** with pre-activation over time at ambient pressure condition (opened system) – grey triangles; at self-pressurized condition (closed system) – blue diamonds.

4. Effect of Various CO Pressures on Reaction Kinetics of **9**, **9-CO**, and **10**

A.

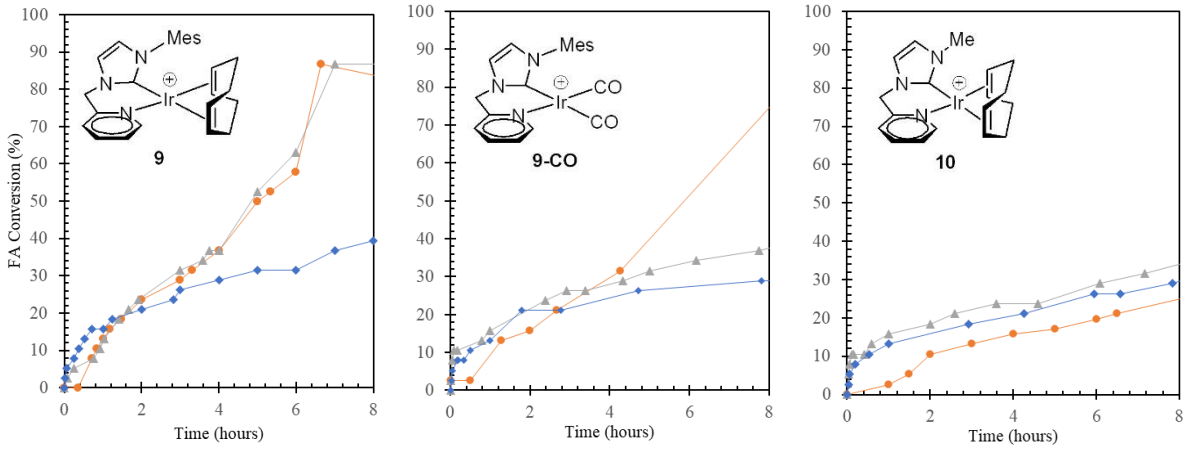

B.

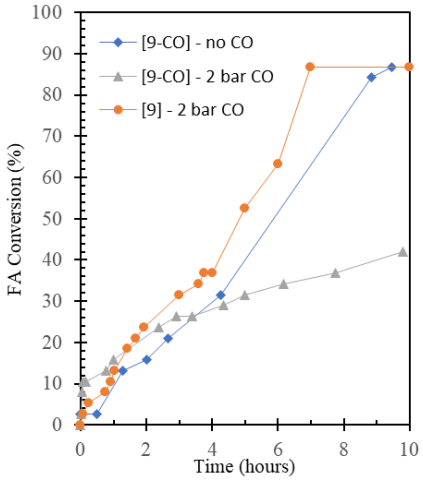

Figure S31. A. Gas evolution of formic acid dehydrogenation by complex **9**, **9-CO**, and **10** over time pretreated with 0 bar CO – orange circles; pretreated with 2 bar CO – grey triangles; pretreated with 8 bar CO – blue diamonds. B. Cross-comparison CO initiation between **9** and **9-CO** showed that after **9** was synthesized in-situ (initiation via catalyst carbonylation), excess CO gas becomes inhibitory to reaction kinetics.

X-ray Crystallography Data

*Crystal structure of **11-CO***

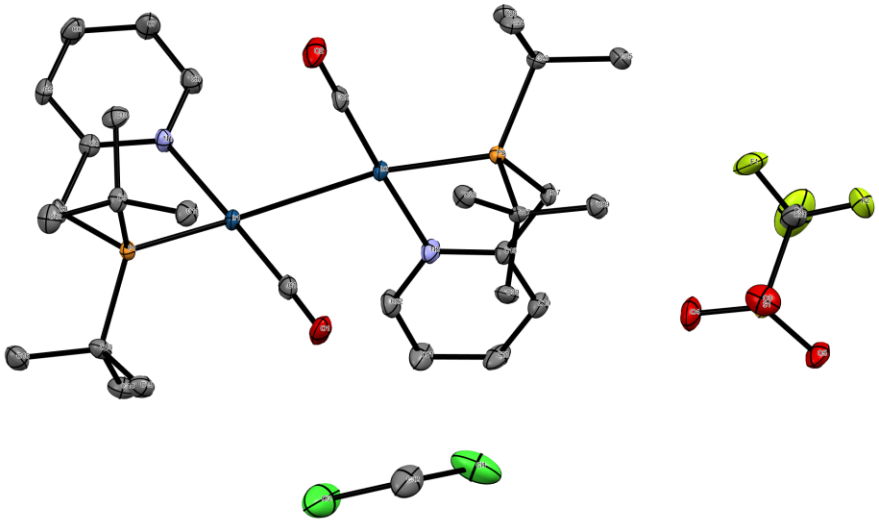

Figure S32. Molecular structure of **11-CO** shown with 50% probability ellipsoids. Hydrogen atoms are omitted for clarity.

A specimen of $C_{32}H_{51}Cl_2F_3Ir_2N_2O_5P_2S$, approximate dimensions 0.030 mm x 0.060 mm x 0.140 mm, was used for the X-ray crystallographic analysis. The X-ray intensity data were measured on a Bruker APEX DUO system equipped with a fine-focus tube (MoKα , λ = 0.71073 Å) and a TRIUMPH curved-crystal monochromator.

The total exposure time was 3.50 hours. The frames were integrated with the Bruker SAINT software package using a SAINT V8.40A (Bruker AXS, 2013) algorithm. The integration of the data using a monoclinic unit cell yielded a total of 100068 reflections to a maximum θ angle of 30.56° (0.70 Å resolution), of which 12322 were independent (average redundancy 8.121, completeness = 99.4%, R_{int} = 7.06%, R_{sig} = 4.33%) and 9871 (80.11%) were greater than $2\sigma(F^2)$. The final cell constants of a = 14.7885(16) Å, b = 17.1958(19) Å, c = 15.9928(18) Å, β = 96.222(2)°, volume = 4043.0(8) $Å^3$, are based upon the refinement of the XYZ-centroids of 9022 reflections above 20 σ(I) with 5.121° < 2θ < 60.94°. Data were corrected for absorption effects using the multi-scan method (SADABS). The ratio of minimum to maximum apparent transmission was 0.762. The calculated minimum and maximum transmission coefficients (based on crystal size) are 0.4450 and 0.8200.

The structure was solved and refined using the Bruker SHELXTL Software Package, using the space group P 1 21/c 1, with Z = 4 for the formula unit, $C_{32}H_{51}Cl_2F_3Ir_2N_2O_5P_2S$. The final anisotropic full-matrix least-squares refinement on F^2 with 458 variables converged at R1 = 2.84%, for the observed data and wR2 = 5.38% for all data. The goodness-of-fit was 1.027. The largest peak in the final difference electron density synthesis was 1.414 e-/Å^3 and the largest hole was -0.995 e-/Å^3 with an RMS deviation of 0.169 e-/Å^3. On the basis of the final model, the calculated density was 1.889 g/cm^3 and F(000), 2232 e-.

Table S1. Sample and crystal data for **11-CO**.

Identification code	Ir2H	
Chemical formula	$C_{32}H_{51}Cl_2F_3Ir_2N_2O_5P_2S$	
Formula weight	1150.05 g/mol	
Temperature	100(2) K	
Wavelength	0.71073 Å	
Crystal size	0.030 x 0.060 x 0.140 mm	
Crystal system	monoclinic	
Space group	P 1 21/c 1	
Unit cell dimensions	a = 14.7885(16) Å	α = 90°
	b = 17.1958(19) Å	β = 96.222(2)°
	c = 15.9928(18) Å	γ = 90°
Volume	4043.0(8) Å^3	
Z	4	
Density (calculated)	1.889 g/cm^3	
Absorption coefficient	6.892 mm^{-1}	
F(000)	2232	

Table S2. Data collection and structure refinement for **11-CO**.

Diffractometer	Bruker APEX DUO
Radiation source	fine-focus tube (MoKα , λ = 0.71073 Å)
Theta range for data collection	1.74 to 30.56°
Index ranges	-20<=h<=21, -24<=k<=24, -22<=l<=22

Reflections collected	100068	
Independent reflections	12322 [R(int) = 0.0706]	
Coverage of independent reflections	99.4%	
Absorption correction	multi-scan	
Max. and min. transmission	0.8200 and 0.4450	
Structure solution technique	direct methods	
Structure solution program	SHELXTL XT 2014/5 (Bruker AXS, 2014)	
Refinement method	Full-matrix least-squares on F^2	
Refinement program	SHELXTL XL 2018/3 (Bruker AXS, 2018)	
Function minimized	$\Sigma\, w(F_o^2 - F_c^2)^2$	
Data / restraints / parameters	12322 / 0 / 458	
Goodness-of-fit on F^2	1.027	
Δ/σ_{max}	0.003	
Final R indices	9871 data; $I>2\sigma(I)$	R1 = 0.0284, wR2 = 0.0494
	all data	R1 = 0.0463, wR2 = 0.0538
Weighting scheme	$w=1/[\sigma^2(F_o^2)+(0.0143P)2+7.3865P]$	
	where $P=(F_o^2+2F_c^2)/3$	
Largest diff. peak and hole	1.414 and -0.995 eÅ^{-3}	
R.M.S. deviation from mean	0.169 eÅ^{-3}	

Table S3. Atomic coordinates and equivalent isotropic atomic displacement parameters (Å^2) for **11-CO**.

	x/a	**y/b**
C1	0.7874(2)	0.1316(2)
C2	0.6307(2)	0.1518(2)
C3	0.8351(2)	0.88721(19)
C4	0.8114(2)	0.91184(19)
C5	0.8064(2)	0.8582(2)
C6	0.7846(3)	0.8816(2)
C7	0.7681(3)	0.9594(2)
C8	0.7742(3)	0.0111(2)
C9	0.6704(2)	0.9262(2)

C10	0.6232(2)	0.9109(2)
C11	0.6202(2)	0.9941(2)
C12	0.6614(3)	0.8530(2)
C13	0.8669(2)	0.9461(2)
C14	0.9581(3)	0.9852(2)
C15	0.8275(3)	0.9870(2)
C16	0.8858(3)	0.8600(2)
C17	0.7390(2)	0.39768(18)
C18	0.8318(2)	0.36783(19)
C19	0.9044(2)	0.4185(2)
C20	0.9888(3)	0.3897(2)
C21	0.9995(3)	0.3102(2)
C22	0.9249(3)	0.2629(2)
C23	0.5570(2)	0.34886(19)
C24	0.4682(2)	0.3076(2)
C25	0.5388(3)	0.4364(2)
C26	0.5886(3)	0.3166(2)
C27	0.6164(2)	0.34935(19)
C28	0.5592(2)	0.2817(2)
C29	0.5636(2)	0.4257(2)
C30	0.7046(2)	0.3552(2)
Ir1	0.79327(2)	0.06799(2)
Ir2	0.72903(2)	0.21430(2)
N1	0.7951(2)	0.98881(16)
N2	0.84175(19)	0.29001(17)
O1	0.7820(2)	0.16911(15)
O2	0.56874(19)	0.11211(15)
P1	0.79013(6)	0.95754(5)
P2	0.64995(6)	0.32717(5)
C31	0.6847(3)	0.6551(2)
F1	0.6333(2)	0.59727(16)
F2	0.6356(2)	0.71982(14)
F3	0.7501(2)	0.66503(17)
O3	0.65813(19)	0.62435(18)

O4	0.7893(2)	0.56646(16)
O5	0.78679(18)	0.70527(15)
S1	0.73585(6)	0.63550(5)
C32	0.9013(3)	0.2899(3)
Cl1	0.93252(9)	0.36751(10)
Cl2	0.97569(9)	0.21009(9)

Table S4. Bond lengths (Å) for **11-CO**.

C1-O1	1.160(4)	C1-Ir1	1.817(4)
C2-O2	1.154(4)	C2-Ir2	1.823(4)
C3-C4	1.496(5)	C3-P1	1.847(3)
C3-H3A	0.99	C3-H3AB	0.99
C4-N1	1.365(4)	C4-C5	1.384(5)
C5-C6	1.383(5)	C5-H5	0.95
C6-C7	1.378(5)	C6-H6	0.95
C7-C8	1.377(5)	C7-H7	0.95
C8-N1	1.361(4)	C8-H8	0.95
C9-C12	1.531(5)	C9-C11	1.538(5)
C9-C10	1.541(5)	C9-P1	1.880(3)
C10-H10A	0.98	C10-H10B	0.98
C10-H10C	0.98	C11-H11A	0.98
C11-H11B	0.98	C11-H11C	0.98
C12-H12A	0.98	C12-H12B	0.98
C12-H12C	0.98	C13-C15	1.537(5)
C13-C14	1.539(5)	C13-C16	1.541(5)
C13-P1	1.871(3)	C14-H14A	0.98
C14-H14B	0.98	C14-H14C	0.98
C15-H15A	0.98	C15-H15B	0.98
C15-H15C	0.98	C16-H16A	0.98
C16-H16B	0.98	C16-H16C	0.98
C17-C18	1.506(5)	C17-P2	1.832(3)
C17-H17A	0.99	C17-H17B	0.99
C18-N2	1.355(4)	C18-C19	1.388(5)

C19-C20	1.375(5)	C19-H19	0.95
C20-C21	1.387(5)	C20-H20	0.95
C21-C22	1.377(5)	C21-H21	0.95
C22-N2	1.354(4)	C22-H22	0.95
C23-C26	1.531(5)	C23-C24	1.537(5)
C23-C25	1.537(5)	C23-P2	1.875(3)
C24-H24A	0.98	C24-H24B	0.98
C24-H24C	0.98	C25-H25A	0.98
C25-H25B	0.98	C25-H25C	0.98
C26-H26A	0.98	C26-H26B	0.98
C26-H26C	0.98	C27-C29	1.533(5)
C27-C28	1.537(5)	C27-C30	1.540(5)
C27-P2	1.873(3)	C28-H28A	0.98
C28-H28B	0.98	C28-H28C	0.98
C29-H29A	0.98	C29-H29B	0.98
C29-H29C	0.98	C30-H30A	0.98
C30-H30B	0.98	C30-H30C	0.98
Ir1-N1	2.124(3)	Ir1-P1	2.2571(9)
Ir1-Ir2	2.8579(3)	Ir1-H1	1.79(4)
Ir2-N2	2.122(3)	Ir2-P2	2.2667(9)
Ir2-H1	1.80(4)	C31-F1	1.319(5)
C31-F2	1.327(5)	C31-F3	1.354(5)
C31-S1	1.820(4)	O3-S1	1.434(3)
O4-S1	1.440(3)	O5-S1	1.438(3)
C32-Cl1	1.750(5)	C32-Cl2	1.761(5)
C32-H32A	0.99	C32-H32B	0.99

Table S5. Bond angles (°) for **11-CO**.

O1-C1-Ir1	176.6(3)	O2-C2-Ir2	179.0(4)
C4-C3-P1	110.5(2)	C4-C3-H3A	109.6
P1-C3-H3A	109.6	C4-C3-H3AB	109.6
P1-C3-H3AB	109.6	H3A-C3-H3AB	108.1
N1-C4-C5	120.8(3)	N1-C4-C3	118.1(3)

C5-C4-C3	121.0(3)	C6-C5-C4	120.6(3)
C6-C5-H5	119.7	C4-C5-H5	119.7
C7-C6-C5	118.6(3)	C7-C6-H6	120.7
C5-C6-H6	120.7	C8-C7-C6	119.2(4)
C8-C7-H7	120.4	C6-C7-H7	120.4
N1-C8-C7	122.8(3)	N1-C8-H8	118.6
C7-C8-H8	118.6	C12-C9-C11	109.6(3)
C12-C9-C10	108.3(3)	C11-C9-C10	107.4(3)
C12-C9-P1	115.5(2)	C11-C9-P1	108.7(2)
C10-C9-P1	107.0(2)	C9-C10-H10A	109.5
C9-C10-H10B	109.5	H10A-C10-H10B	109.5
C9-C10-H10C	109.5	H10A-C10-H10C	109.5
H10B-C10-H10C	109.5	C9-C11-H11A	109.5
C9-C11-H11B	109.5	H11A-C11-H11B	109.5
C9-C11-H11C	109.5	H11A-C11-H11C	109.5
H11B-C11-H11C	109.5	C9-C12-H12A	109.5
C9-C12-H12B	109.5	H12A-C12-H12B	109.5
C9-C12-H12C	109.5	H12A-C12-H12C	109.5
H12B-C12-H12C	109.5	C15-C13-C14	107.9(3)
C15-C13-C16	109.7(3)	C14-C13-C16	108.1(3)
C15-C13-P1	111.1(2)	C14-C13-P1	107.7(2)
C16-C13-P1	112.2(2)	C13-C14-H14A	109.5
C13-C14-H14B	109.5	H14A-C14-H14B	109.5
C13-C14-H14C	109.5	H14A-C14-H14C	109.5
H14B-C14-H14C	109.5	C13-C15-H15A	109.5
C13-C15-H15B	109.5	H15A-C15-H15B	109.5
C13-C15-H15C	109.5	H15A-C15-H15C	109.5
H15B-C15-H15C	109.5	C13-C16-H16A	109.5
C13-C16-H16B	109.5	H16A-C16-H16B	109.5
C13-C16-H16C	109.5	H16A-C16-H16C	109.5
H16B-C16-H16C	109.5	C18-C17-P2	111.4(2)
C18-C17-H17A	109.3	P2-C17-H17A	109.3
C18-C17-H17B	109.3	P2-C17-H17B	109.3
H17A-C17-H17B	108.0	N2-C18-C19	121.6(3)

N2-C18-C17	117.5(3)	C19-C18-C17	120.9(3)
C20-C19-C18	119.7(3)	C20-C19-H19	120.1
C18-C19-H19	120.1	C19-C20-C21	119.2(3)
C19-C20-H20	120.4	C21-C20-H20	120.4
C22-C21-C20	118.4(4)	C22-C21-H21	120.8
C20-C21-H21	120.8	N2-C22-C21	123.2(3)
N2-C22-H22	118.4	C21-C22-H22	118.4
C26-C23-C24	108.5(3)	C26-C23-C25	108.3(3)
C24-C23-C25	109.4(3)	C26-C23-P2	106.5(2)
C24-C23-P2	111.0(2)	C25-C23-P2	113.0(2)
C23-C24-H24A	109.5	C23-C24-H24B	109.5
H24A-C24-H24B	109.5	C23-C24-H24C	109.5
H24A-C24-H24C	109.5	H24B-C24-H24C	109.5
C23-C25-H25A	109.5	C23-C25-H25B	109.5
H25A-C25-H25B	109.5	C23-C25-H25C	109.5
H25A-C25-H25C	109.5	H25B-C25-H25C	109.5
C23-C26-H26A	109.5	C23-C26-H26B	109.5
H26A-C26-H26B	109.5	C23-C26-H26C	109.5
H26A-C26-H26C	109.5	H26B-C26-H26C	109.5
C29-C27-C28	109.5(3)	C29-C27-C30	108.4(3)
C28-C27-C30	108.6(3)	C29-C27-P2	114.0(2)
C28-C27-P2	109.2(2)	C30-C27-P2	107.2(2)
C27-C28-H28A	109.5	C27-C28-H28B	109.5
H28A-C28-H28B	109.5	C27-C28-H28C	109.5
H28A-C28-H28C	109.5	H28B-C28-H28C	109.5
C27-C29-H29A	109.5	C27-C29-H29B	109.5
H29A-C29-H29B	109.5	C27-C29-H29C	109.5
H29A-C29-H29C	109.5	H29B-C29-H29C	109.5
C27-C30-H30A	109.5	C27-C30-H30B	109.5
H30A-C30-H30B	109.5	C27-C30-H30C	109.5
H30A-C30-H30C	109.5	H30B-C30-H30C	109.5
C1-Ir1-N1	176.55(13)	C1-Ir1-P1	94.30(11)
N1-Ir1-P1	82.84(8)	C1-Ir1-Ir2	74.08(11)
N1-Ir1-Ir2	107.89(8)	P1-Ir1-Ir2	156.60(2)

C1-Ir1-H1	97.3(13)	N1-Ir1-H1	85.9(13)
P1-Ir1-H1	165.3(13)	Ir2-Ir1-H1	37.5(13)
C2-Ir2-N2	177.44(14)	C2-Ir2-P2	96.16(11)
N2-Ir2-P2	82.42(8)	C2-Ir2-Ir1	78.16(11)
N2-Ir2-Ir1	104.03(8)	P2-Ir2-Ir1	154.48(2)
C2-Ir2-H1	97.6(13)	N2-Ir2-H1	83.5(13)
P2-Ir2-H1	164.7(13)	Ir1-Ir2-H1	37.3(13)
C8-N1-C4	118.0(3)	C8-N1-Ir1	122.1(2)
C4-N1-Ir1	119.7(2)	C22-N2-C18	117.8(3)
C22-N2-Ir2	121.6(2)	C18-N2-Ir2	120.6(2)
C3-P1-C13	103.90(15)	C3-P1-C9	106.41(16)
C13-P1-C9	112.01(16)	C3-P1-Ir1	100.64(11)
C13-P1-Ir1	120.21(11)	C9-P1-Ir1	111.70(11)
C17-P2-C27	105.58(15)	C17-P2-C23	103.85(15)
C27-P2-C23	112.67(15)	C17-P2-Ir2	100.73(11)
C27-P2-Ir2	111.55(11)	C23-P2-Ir2	120.25(11)
F1-C31-F2	108.8(4)	F1-C31-F3	106.3(3)
F2-C31-F3	106.7(3)	F1-C31-S1	112.5(3)
F2-C31-S1	111.8(3)	F3-C31-S1	110.4(3)
O3-S1-O5	114.76(18)	O3-S1-O4	114.40(18)
O5-S1-O4	115.55(17)	O3-S1-C31	102.79(19)
O5-S1-C31	102.88(18)	O4-S1-C31	104.11(19)
Cl1-C32-Cl2	112.6(3)	Cl1-C32-H32A	109.1
Cl2-C32-H32A	109.1	Cl1-C32-H32B	109.1
Cl2-C32-H32B	109.1	H32A-C32-H32B	107.8

Table S6. Torsion angles (°) for **11-CO**.

P1-C3-C4-N1	24.4(4)	P1-C3-C4-C5	-155.7(3)
N1-C4-C5-C6	0.0(5)	C3-C4-C5-C6	-179.8(3)
C4-C5-C6-C7	0.0(6)	C5-C6-C7-C8	0.3(6)
C6-C7-C8-N1	-0.7(6)	P2-C17-C18-N2	20.9(4)

P2-C17-C18-C19	-159.5(3)	N2-C18-C19-C20	0.4(5)
C17-C18-C19-C20	-179.1(3)	C18-C19-C20-C21	-1.2(6)
C19-C20-C21-C22	0.7(6)	C20-C21-C22-N2	0.7(6)
C7-C8-N1-C4	0.7(5)	C7-C8-N1-Ir1	-174.8(3)
C5-C4-N1-C8	-0.4(5)	C3-C4-N1-C8	179.5(3)
C5-C4-N1-Ir1	175.2(3)	C3-C4-N1-Ir1	-4.9(4)
C21-C22-N2-C18	-1.5(6)	C21-C22-N2-Ir2	-179.8(3)
C19-C18-N2-C22	0.9(5)	C17-C18-N2-C22	-179.6(3)
C19-C18-N2-Ir2	179.3(3)	C17-C18-N2-Ir2	-1.2(4)
C4-C3-P1-C13	-154.6(2)	C4-C3-P1-C9	87.0(3)
C4-C3-P1-Ir1	-29.6(3)	C15-C13-P1-C3	-167.5(2)
C14-C13-P1-C3	74.5(3)	C16-C13-P1-C3	-44.3(3)
C15-C13-P1-C9	-53.0(3)	C14-C13-P1-C9	-171.1(2)
C16-C13-P1-C9	70.1(3)	C15-C13-P1-Ir1	81.1(3)
C14-C13-P1-Ir1	-36.9(3)	C16-C13-P1-Ir1	-155.7(2)
C12-C9-P1-C3	72.9(3)	C11-C9-P1-C3	-163.5(2)
C10-C9-P1-C3	-47.8(3)	C12-C9-P1-C13	-40.0(3)
C11-C9-P1-C13	83.6(3)	C10-C9-P1-C13	-160.7(2)
C12-C9-P1-Ir1	-178.2(2)	C11-C9-P1-Ir1	-54.6(3)
C10-C9-P1-Ir1	61.1(2)	C18-C17-P2-C27	88.4(3)
C18-C17-P2-C23	-152.8(2)	C18-C17-P2-Ir2	-27.8(2)
C29-C27-P2-C17	70.8(3)	C28-C27-P2-C17	-166.5(2)
C30-C27-P2-C17	-49.1(3)	C29-C27-P2-C23	-41.9(3)
C28-C27-P2-C23	80.8(3)	C30-C27-P2-C23	-161.8(2)
C29-C27-P2-Ir2	179.3(2)	C28-C27-P2-Ir2	-58.0(2)
C30-C27-P2-Ir2	59.4(2)	C26-C23-P2-C17	74.7(3)
C24-C23-P2-C17	-167.4(2)	C25-C23-P2-C17	-44.2(3)
C26-C23-P2-C27	-171.6(2)	C24-C23-P2-C27	-53.7(3)
C25-C23-P2-C27	69.6(3)	C26-C23-P2-Ir2	-36.8(3)
C24-C23-P2-Ir2	81.1(2)	C25-C23-P2-Ir2	-155.6(2)
F1-C31-S1-O3	-59.8(4)	F2-C31-S1-O3	63.1(3)
F3-C31-S1-O3	-178.3(3)	F1-C31-S1-O5	-179.3(3)
F2-C31-S1-O5	-56.4(3)	F3-C31-S1-O5	62.2(3)
F1-C31-S1-O4	59.8(4)	F2-C31-S1-O4	-177.3(3)

F3-C31-S1-O4	-58.7(3)

Table S7. Anisotropic atomic displacement parameters ($Å^2$) for **11-CO**.

The anisotropic atomic displacement factor exponent takes the form: $-2\pi^2[h^2 a^{*2} U_{11} + ... + 2 h k a^* b^* U_{12}]$

	U_{11}	U_{22}	U_{33}	U_{23}	U_{13}	U_{12}
C1	0.0198(18)	0.0116(16)	0.0219(18)	0.0029(14)	0.0013(15)	-0.0001(14)
C2	0.0168(18)	0.0119(16)	0.027(2)	0.0003(14)	0.0019(15)	0.0066(14)
C3	0.0166(17)	0.0101(15)	0.0164(17)	0.0004(12)	0.0047(13)	0.0063(13)
C4	0.0143(16)	0.0145(16)	0.0150(16)	0.0000(13)	0.0047(13)	-0.0001(13)
C5	0.0241(19)	0.0094(15)	0.0231(19)	-0.0010(14)	0.0042(15)	0.0010(14)
C6	0.041(2)	0.0198(19)	0.0181(19)	-0.0049(15)	0.0054(17)	0.0003(17)
C7	0.050(3)	0.0210(19)	0.0139(18)	0.0002(15)	0.0010(18)	0.0024(19)
C8	0.025(2)	0.0189(18)	0.0189(18)	0.0049(14)	0.0027(15)	0.0027(15)
C9	0.0129(16)	0.0142(16)	0.0204(17)	-0.0008(14)	0.0054(13)	0.0016(13)
C10	0.0176(18)	0.0217(18)	0.0217(19)	-0.0013(15)	0.0013(15)	-0.0067(15)
C11	0.0151(17)	0.0199(18)	0.0246(19)	-0.0039(15)	0.0048(15)	0.0021(14)
C12	0.0224(19)	0.0192(18)	0.0242(19)	0.0017(15)	0.0090(16)	-0.0009(15)
C13	0.0151(17)	0.0194(17)	0.0126(16)	0.0009(13)	0.0003(13)	0.0016(14)
C14	0.0182(19)	0.029(2)	0.0222(19)	0.0005(16)	-0.0024(15)	0.0003(16)
C15	0.0215(19)	0.0252(19)	0.0146(17)	-0.0008(15)	0.0020(15)	0.0023(16)
C16	0.027(2)	0.0236(19)	0.0187(18)	0.0028(15)	0.0008(16)	0.0065(16)
C17	0.0132(16)	0.0080(14)	0.0212(18)	0.0011(13)	0.0014(14)	-0.0008(12)
C18	0.0129(16)	0.0134(16)	0.0185(17)	-0.0015(13)	0.0044(14)	0.0009(13)
C19	0.0183(18)	0.0139(16)	0.0252(19)	-0.0042(14)	0.0046(15)	-0.0021(14)
C20	0.0138(18)	0.0234(19)	0.034(2)	-0.0094(17)	0.0030(16)	-0.0060(15)
C21	0.0117(17)	0.023(2)	0.043(3)	-0.0077(18)	0.0005(17)	0.0034(15)
C22	0.0181(18)	0.0166(17)	0.032(2)	-0.0020(15)	0.0028(16)	0.0067(14)
C23	0.0137(16)	0.0130(15)	0.0133(16)	-0.0007(13)	-0.0021(13)	0.0014(13)
C24	0.0159(17)	0.0200(18)	0.0209(18)	-0.0005(14)	-0.0039(14)	-0.0002(14)
C25	0.0221(18)	0.0167(17)	0.0177(17)	0.0018(14)	-0.0033(14)	0.0031(15)
C26	0.028(2)	0.0191(18)	0.0122(16)	-0.0015(14)	-0.0010(15)	0.0031(15)
C27	0.0162(16)	0.0118(15)	0.0098(15)	-0.0014(12)	-0.0009(13)	0.0013(13)

C28	0.0225(18)	0.0173(17)	0.0133(16)	0.0039(14)	0.0044(14)	-0.0023(15)
C29	0.0193(18)	0.0181(17)	0.0175(17)	-0.0001(14)	0.0032(14)	0.0054(14)
C30	0.0200(18)	0.0230(18)	0.0145(16)	-0.0045(15)	-0.0046(14)	0.0078(15)
Ir1	0.01283(6)	0.00803(6)	0.01419(6)	-0.00036(5)	0.00234(5)	0.00127(5)
Ir2	0.01194(6)	0.00784(6)	0.01507(6)	-0.00050(5)	0.00226(5)	0.00100(5)
N1	0.0197(15)	0.0122(13)	0.0132(14)	0.0020(11)	0.0045(12)	0.0020(12)
N2	0.0136(14)	0.0136(14)	0.0239(16)	-0.0030(12)	0.0033(12)	0.0017(12)
O1	0.0412(18)	0.0160(13)	0.0230(14)	-0.0061(11)	0.0055(13)	0.0022(12)
O2	0.0212(15)	0.0177(14)	0.0514(19)	-0.0046(13)	-0.0009(13)	-0.0040(11)
P1	0.0119(4)	0.0093(4)	0.0123(4)	-0.0007(3)	0.0023(3)	0.0021(3)
P2	0.0106(4)	0.0088(4)	0.0122(4)	-0.0002(3)	0.0015(3)	0.0000(3)
C31	0.044(3)	0.024(2)	0.0174(19)	-0.0020(16)	-0.0009(18)	-0.0041(19)
F1	0.093(3)	0.0321(15)	0.0386(16)	-0.0003(12)	-0.0337(16)	-0.0232(16)
F2	0.0638(19)	0.0237(13)	0.0358(15)	0.0068(11)	-0.0136(13)	0.0081(13)
F3	0.107(3)	0.0476(18)	0.0370(17)	-0.0072(14)	0.0396(18)	-0.0135(18)
O3	0.0239(15)	0.0428(18)	0.0320(16)	0.0076(14)	0.0064(13)	-0.0045(13)
O4	0.0305(16)	0.0165(14)	0.055(2)	-0.0066(13)	-0.0002(15)	0.0078(12)
O5	0.0198(14)	0.0190(14)	0.0418(17)	-0.0076(12)	-0.0037(12)	-0.0034(11)
S1	0.0162(4)	0.0129(4)	0.0232(5)	-0.0016(3)	-0.0006(4)	-0.0001(3)
C32	0.023(2)	0.038(3)	0.052(3)	-0.012(2)	0.005(2)	0.0004(19)
Cl1	0.0410(7)	0.0929(11)	0.0357(7)	0.0189(7)	-0.0006(6)	0.0025(7)
Cl2	0.0420(7)	0.0600(9)	0.0840(11)	-0.0333(8)	-0.0186(7)	0.0204(7)

Table S8. Hydrogen atomic coordinates and isotropic atomic displacement parameters ($Å^2$) for **11-CO**.

	x/a	**y/b**	**z/c**	**U(eq)**
H3A	0.9021	-0.1163	0.4655	0.017
H3AB	0.8092	-0.1649	0.4617	0.017
H5	0.8180	-0.1952	0.3110	0.023
H6	0.7811	-0.1551	0.1717	0.031
H7	0.7528	-0.0230	0.1442	0.034
H8	0.7634	0.0647	0.2545	0.025
H10A	0.6274	-0.0425	0.4134	0.031
H10B	0.5590	-0.1018	0.4512	0.031

H10C	0.6530	-0.1327	0.4227	0.031
H11A	0.6193	0.0390	0.5366	0.03
H11B	0.6517	0.0082	0.6295	0.03
H11C	0.5576	-0.0216	0.5811	0.03
H12A	0.5970	-0.1611	0.5889	0.032
H12B	0.6867	-0.1370	0.6484	0.032
H12C	0.6947	-0.1899	0.5672	0.032
H14A	0.9843	-0.0395	0.5661	0.035
H14B	1.0002	-0.0206	0.6646	0.035
H14C	0.9481	0.0405	0.6011	0.035
H15A	0.8135	0.0412	0.6837	0.031
H15B	0.8721	-0.0145	0.7489	0.031
H15C	0.7717	-0.0396	0.7109	0.031
H16A	0.9133	-0.1654	0.6020	0.035
H16B	0.8285	-0.1661	0.6562	0.035
H16C	0.9275	-0.1433	0.6997	0.035
H17A	0.7373	0.4085	0.3049	0.017
H17B	0.7271	0.4470	0.3945	0.017
H19	0.8957	0.4729	0.4091	0.023
H20	1.0391	0.4238	0.4567	0.028
H21	1.0570	0.2890	0.4777	0.032
H22	0.9322	0.2085	0.4479	0.027
H24A	0.4234	0.3138	0.2633	0.029
H24B	0.4445	0.3306	0.3619	0.029
H24C	0.4802	0.2522	0.3228	0.029
H25A	0.5954	0.4628	0.2751	0.029
H25B	0.5162	0.4577	0.3355	0.029
H25C	0.4933	0.4445	0.2364	0.029
H26A	0.5431	0.3287	0.1682	0.03
H26B	0.5959	0.2601	0.2205	0.03
H26C	0.6469	0.3403	0.2062	0.03
H28A	0.5028	0.2772	0.4808	0.026
H28B	0.5444	0.2917	0.5761	0.026
H28C	0.5939	0.2332	0.5178	0.026

H29A	0.5983	0.4683	0.4731	0.027
H29B	0.5541	0.4363	0.5534	0.027
H29C	0.5045	0.4212	0.4608	0.027
H30A	0.7398	0.3072	0.5474	0.029
H30B	0.6895	0.3626	0.6080	0.029
H30C	0.7407	0.3994	0.5342	0.029
H32A	0.8389	0.2730	0.6963	0.045
H32B	0.9004	0.3079	0.7760	0.045
H1	0.816(3)	0.142(2)	0.375(2)	0.029(11)

Table S9. CO Reformation of **10**

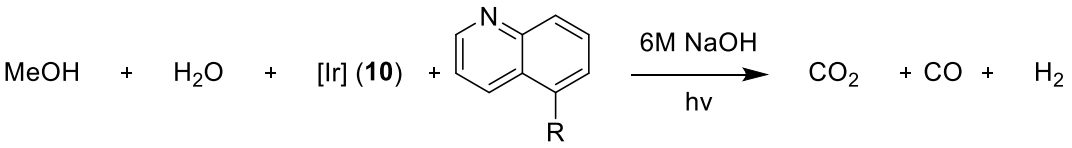

40 ppm	5 mol%, R = CN	–	33%
40 ppm	5 mol%, R = OMe	–	trace
0 ppm	5 mol%, R = CN	–	13%

Conditions: 1 mL MeOH, 3 mL H_2O, 300 nm hv, room temp. CO collected as $NaCO_3$. No reaction observed without hv, NaOH, and quinoline all present.